24th Mediterranean Conference on Control and Automation (MED)
June 21-24, 2016, Athens, Greece

Control Strategies Applied in the HYSOL Demonstrator: a Simulation-Based Evaluation*

Lidia Roca[1], Javier Bonilla[1], Manuel Berenguel[2], Lucía González[3] and Alberto R.Rocha[4]

***Abstract*— HYSOL project was born under the idea of designing a new hybrid concentrating solar power plant concept fully based on renewable energies and able to provide stable power. Within this project, one of the main activities is the development of a demonstrator facility to evaluate experimentally the gas turbine heat recovery and its transference to a molten-salt storage system. This paper describes the main control loops proposed to maintain the facility at different operating points to study both nominal and off-design states.**

I. INTRODUCTION

The stability and reliability of power supply is an important challenge in Concentrating Solar Power plants (CSP) that can be relieved by incorporating Thermal Energy Storage (TES) or different energy sources in a hybrid plant. This last option has its main exponent in the Integrated Solar Combined Cycle plants (ISCC) which usually includes a CSP plant, a conventional Combined Cycle (CC) and a heat recovery steam generator. In order to increase the solar contribution, some new hybrid designs have been proposed [7]. HYSOL project emerges from the idea of designing a CSP plant fully renewable and able to guarantee power stability. One of the key elements in this new design is the operation optimization to produce electrical energy to satisfy the demand curves but reducing costs and maximizing the use of the solar energy. Moreover, due to the hybrid nature of the system, startups and shutdowns must be treated as special optimization problems to reduce operating times while maintaining the system in safety conditions. Similar optimization problems can be found for the case of CC plants [6] in which the main goal is to reduce the startup and shutdown times considering thermal gradient constraints.
Nevertheless, previous to develop a hierarchical control structure with an economic optimization in the top layer, the regulatory layer to control the main involved variables must be designed and tested. This paper describes the first step towards the HYSOL configuration automation, showing the main control loops in a demonstrator plant and evaluating these controllers in simulation. Section II resumes the HYSOL project, Section III explains the control loops defined in the demonstrator plant, the dynamic models are presented in Section IV and simulations are discussed in Section V. The paper ends with the conclusions obtained from this work.

*This research has been funded by the EU 7th Framework Programme (Theme Energy 2012.2.5.2) under grant agreement 308912 - HYSOL project - Innovative Configuration of a Fully Renewable Hybrid CSP Plant, the Spanish Ministry of Economy and Competitiveness through ERDF and PLAN E funds (C.N. SolarNOVA ICT-CEPU 2009-02).

[1]Lidia Roca and Javier Bonilla are with the Plataforma Solar de Almería - CIEMAT, CIESOL, Tabernas, Almería, Spain, lidia.roca@psa.es, javier.bonilla@psa.es

[2]Manuel Berenguel with the University of Almería, CIESOL - ceiA3, Spain, beren@ual.es

[3] Lead Engineer, ACS/Cobra T&I, Madrid, Spain

[4] Head of Technology and Innovation, ACS/Cobra T&I, Madrid, Spain

II. HYSOL PROJECT

The HYSOL project - *Innovative Configuration of a Fully Renewable Hybrid CSP Plant* from the EU 7^{th} Framework Programme is in the *Theme Energy 2012.2.5.2 - hybridization of CSP with other energy sources*. The HYSOL consortium is composed of partners from four European countries, defining a multidisciplinary team, with partners devoted to research activities: CIEMAT-PSA, ENEA, UPM, DTU/MAN/SYS and SDLO-PRI, together with industrial partners: ACS/Cobra, AITESA and IDIE. The project coordinator and promoter is ACS/Cobra, a company with a vast experience in the development, building, operation and maintenance of industrial facilities and power plants.

A. HYSOL Technology

The HYSOL project focuses in the development of a innovative configuration based on a CSP plant with a molten salt thermal TES system, steam turbine (a Rankine cycle, if an ideal cycle is considered), gas turbine (an open Brayton cycle) and a flue gas - molten salt Heat Recovery System (HRS). One of the proposed HYSOL schemes is shown in Fig. 1.

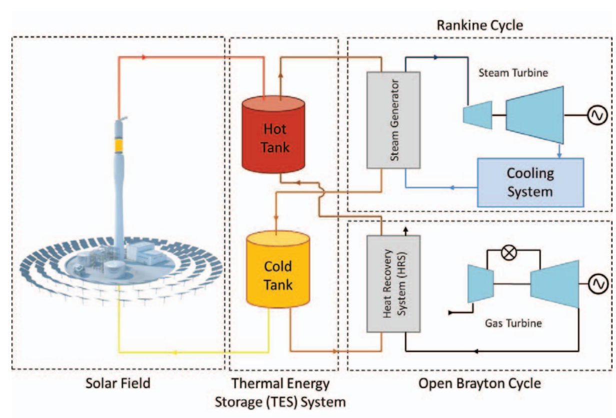

Fig. 1. HYSOL configuration with tower solar thermal power plant and direct TES

Nevertheless, there are several HYSOL configurations, since the HYSOL concept can be applied to parabolic trough collectors (PTC) or tower solar thermal power plants with direct or indirect TES systems. The HYSOL concept depicted in Fig. 1 corresponds to a tower solar thermal power plant with direct TES, where the working fluid, as well as the storage fluid, is molten salt. There are mainly three operating modes; they are briefly summarized as follows.

1) Molten salt thermal energy from the solar field is stored in the hot molten salt tank; this energy is used to produced electricity by means of a steam generator in a Rankine cycle, whereas the energy excess is kept in the hot tank. The steam generator outlet molten salts are stored in the cold tank.
2) When the solar field cannot provide enough energy to maintain the steam turbine nominal operating conditions and the TES system has enough thermal energy, molten salt keeps flowing from the hot tank to the steam generator as described in point 1.
3) When the solar field, as well as the TES system, cannot provide enough thermal energy to the Rankine cycle, the gas turbine in the open Brayton cycle will produce electricity. Furthermore, the turbine flue gases will be used to heat molten salt from the cold tank in the HRS. The hot molten salt coming from the HRS will be stored in the hot tank, which will be used again in the Rankine cycle as described in point 2. Additionally, the flue gases from the HRS can be used to optimize the plant performance.

B. HYSOL Demonstrator

The Manchasol solar thermal power plant, owned by ACS/Cobra, is currently being adapted as a demonstrator of the HYSOL technology. The demonstrator focuses in the gas-molten salt HRS, an sketch of it is shown in Fig. 2. Its main components are briefly introduced in the following lines.

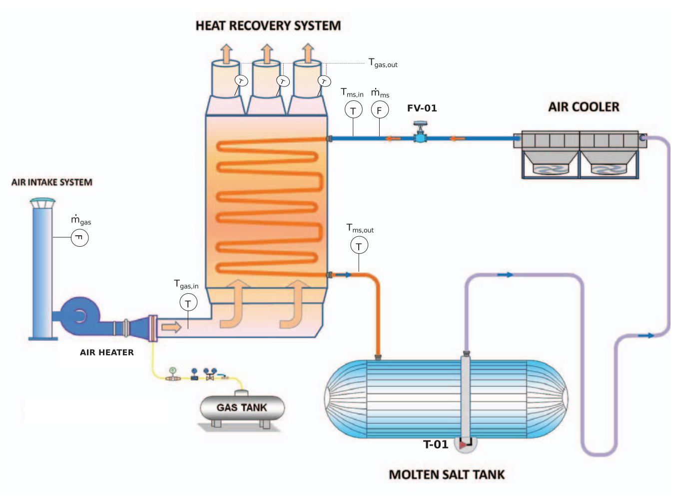

Fig. 2. HYSOL demonstrator configuration

- *Virtual gas turbine.* This component, with the appropriate control system, emulates a gas turbine with afterheater like the one considered in the HYSOL configuration. This element is composed by an air intake system, a gas tank, and an air heater, (see Fig. 2).
- *Heat Recovery System (HRS).* The HRS allows to recover thermal energy from the virtual gas turbine flue gases, thus heating molten salts in the same ways as in the HYSOL configuration.
- *Molten salt tank.* Once molten salts are heated in the HRS, they are stored in this tank, therefore this tank emulates the hot molten salt tank.
- *Air cooler.* Since there is only one tank in the demonstrator, an air cooler emulates the molten salt discharging process, i.e. the energy transfer from the hot tank molten salt in the steam generator.

C. Operation

The normal operation of the demonstrator plant must follow manufacturer constraints to guarantee the security of the HRS:

- Startup: Following the manufacturer's startup path, the facility must be prepared to accomplish these steps:
  1) Startup following a gas turbine curve.
  2) Once the gas temperature at the inlet of the HRS reaches 350 °C, this temperature is maintained.
  3) Once the gas temperature at the outlet of the HRS reaches 300 °C, the exchanger tubes can be filled up with the salts and the startup goes on following the turbine curve.
- Shutdown: When the virtual gas turbine is stopped, the afterheater must assure a gas temperature at the inlet of the HRS to maintain the temperature gradient below the maximum allowed.

III. CONTROL LOOPS

A. Hot molten salt temperature control

The objective is to maintain the hot molten salts temperature, $T_{ms,out}$ (see Fig.2), in its nominal value, 560 °C, (or in another value to validate the static and dynamic models) under different operating conditions in the demonstrator. Two different cases will be considered:

- Temperature control with molten salts mass flow rate as control variable.
- Temperature control with gas mass flow rate as control variable. This case will not be included in real plants, but it is considered to perform off-design tests to validate static and dynamic models.

1) Control variable: molten salt mass flow rate: The scheme proposed is shown in Fig. 3. The slave control is in charge of regulating the valve aperture, u_{V1}, to achieve the desired molten salts mass flow rate, $\dot{m}_{ms}$. The master control combines a classical feedback action (PI controller with anti-windup [1]) and a feedforward action (FF) which provides the operating point [2]. The output of the feedforward action, $\dot{m}_{ms,FF}$, is considered in the feedback action to modify on-line the saturation limits included in the anti-windup action.

The feedforward action is obtained from an stationary energy balance in the HRS neglecting heat losses:

$$c_{p,ms} \cdot (T_{ms,out} - T_{ms,in}) \cdot \dot{m}_{ms} = \quad (1)$$
$$c_{p,gas} \cdot (T_{gas,in} - T_{gas,out}) \cdot \dot{m}_{gas} \quad (2)$$

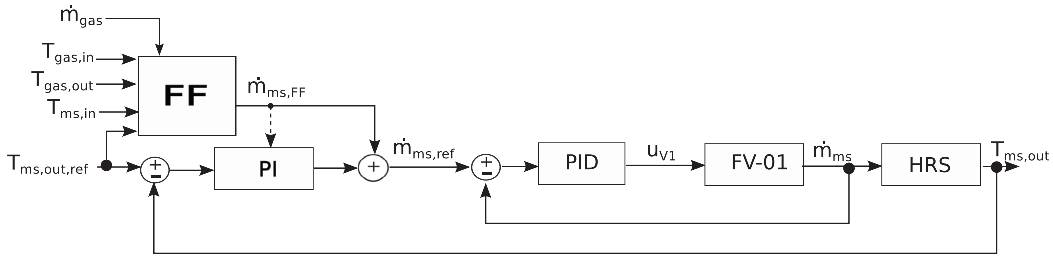

Fig. 3. Molten salt temperature control using the molten salt mass flow rate.

2) Control variable: gas mass flow rate: The scheme proposed is shown in Fig. 4. This controller also combines a PI with a feedforward action (FF). This combination provides the gas temperature setpoint, $\dot{m}_{gas,ref}$, which will be sent to the gas heater device.

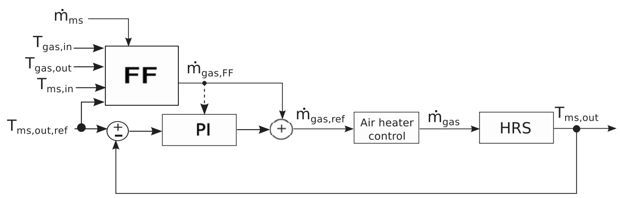

Fig. 4. Molten salt temperature control using the gas mass flow rate

The feedforward action is obtained from the previous stationary energy balance (1).

B. Air heater

The air heater device in charge of emulating the behavior of the exhaust gases from the turbine includes local controllers to maintain the temperature and mass flow rate of the outlet flue gases at desired values that can be modified easily from the SCADA. Nevertheless, it is important to evaluate experimentally the performance of these controllers and include, if necessary, an external control loop to improve them. In this case, the external controller will be used to manage the setpoints which are commanded to the air heater and blower controllers.

C. Molten salt pump

As commented in Section III-A, the molten salt mass flow rate is controlled with the aperture of valve FV-01. But these aperture changes affect the performance of the molten salt pump located inside the tank T-01. To avoid operating points that could damage the pump, the option tested in other solar plants, such as the case described in [8] is to design a pump speed controller to maintain a specific pressure drop in the valve that regulates the liquid flow rate. This pressure drop setpoint can be calculated to minimize the power consumption. This optimization research line can be found in water distribution systems and air conditioning systems [4]. In the HYSOL demonstrator, the objective of the molten salt pump control is to maintain the pump operating point close to the maximum value of the efficiency curve (η) using the speed variable as control variable. Previously, it will necessary to obtain experimentally the relation between the molten salt volumetric flow rate, $\dot{q}_{ms}$, the valve aperture, u_{v1}, and pump speed values, u_{PS}. With the obtained volumetric flow rate values and, following the manufacturer pump curves, a collection of parametric functions will be obtained:

$$\eta_i = \theta_{i,1} \cdot q_{ms}^2 + \theta_{i,2} \cdot q_{ms} + \theta_{i,3}, \tag{3}$$

where θ are the fit coefficients, $i = 1, 2, ..., l$ and l is the number of the representative equations obtained at different valve apertures.

Fig. 5 shows the proposed controller. The estimator block calculates the estimated efficiency, η_e, from eq. (3) while a gain-scheduling P controller provides the pump speed. Since the objective is to maintain the efficiency around its maximum $[\eta_{max} - \Delta\eta, \eta_{max}]$, a dead zone block is included to avoid pump speed variations if $\eta_e \geq \eta_{max} - \Delta\eta$.

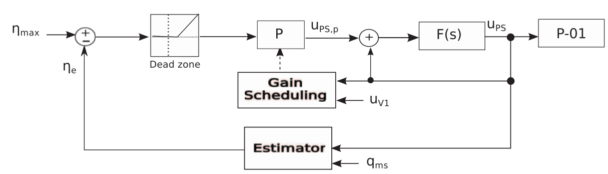

Fig. 5. Pump control efficiency

Notice that the system composed by the valve and the molten salt pump is a MIMO one with two inputs (u_{V1}, u_{PS}) and two outputs $(\eta, \dot{m}_{ms})$. With the aim of non-affecting the molten salt mass flow rate controller, a smooth response in the pump control loop has been imposed including a filter $F(s)$. Nevertheless, when the first experiments will be carried out at the demonstrator facility, the dynamic models of the valve and pump will be obtained to study the coupling of the outputs as a consequence of variations in the two inputs. From the obtained results, the option of developing a gain-scheduling multivariable controller will be studied.

IV. HYSOL DEMONSTRATOR MODELS

To test the startup operation (see Section II-C) and the proposed controllers described in Section III-A, dynamic models of the main components of the HYSOL demonstrator facility have been developed. This section describes briefly these models.

A. HRS model

To model the HRS, the Modelica language and Dymola tool have been used. The main components of the system have been modeled and developed in a reusable library for the HYSOL project. Fig. 6 shows the icon of the model, being the inputs the mass flow rates and inlet temperatures of molten salts and exhaust gases, and outlet pressures to close the hydraulic circuits. There are two versions of the model, in the detailed one, the speed velocity and ambient temperature are also inputs. With these inputs the model calculates the exchanged heat and provides the outlet temperatures of both molten salt and gases.

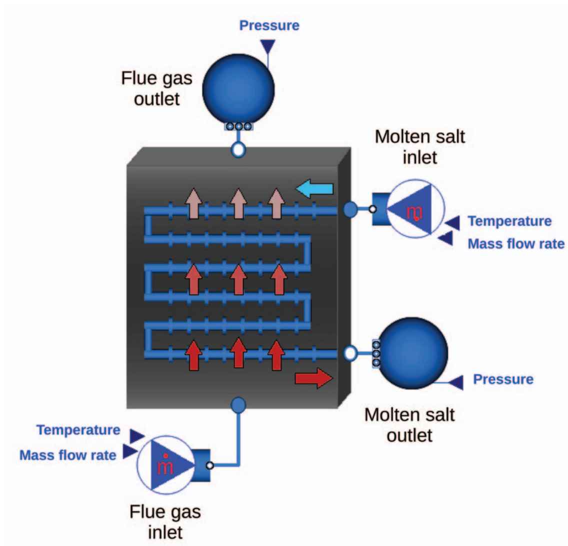

Fig. 6. Heat recovery system model icon and inputs

B. Virtual gas turbine

As commented in Section II-B, the air heater device must simulate the behavior of the exhaust gases from a gas turbine working with an afterheater. Following the manufacturer technical characteristics, a first-order model;

$$H(s) = \frac{11.84}{10s + 1} \tag{4}$$

has been proposed to model the gas temperature increment, $T_{h,out} - T_{h,in}$, as a function of the heater load, n_h, (0-100%). Fig. 7 shows an scheme of the virtual gas turbine. Different exhaust gases temperature and mass flow rate curves can be loaded in the HYSOL SCADA to simulate warm and cold startups [5], shutdowns and partial loads [3]. To increase the exhaust gases temperature, $T_{exh,out}$, and reach the HRS inlet gas design temperature, $T_{ah,ref}$, a virtual afterheater with a PID controller is considered. For the sake of simplicity, the dynamics of this heater will be considered such as the air heater one (4). The simulated $T_{gas,ref}$ is the setpoint which enters to the real air heater device which must increase the temperature of the air, T_{amb}. In this paper, the air heater device is modeled including a PID controller, so that the model provides the final gas temperature that enters the HRS, $T_{gas,in}$.

The afterheater load, n_v, will be useful to carry on future studies about the gas consumption that this technology involves.

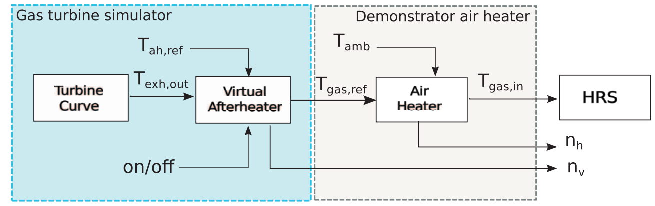

Fig. 7. Virtual gas turbine: gas turbine simulator and demonstrator air heater.

V. SIMULATION RESULTS

The startup operation and the control loops presented in Section III-A have been evaluated in simulation using the dynamic models of the HRS developed under the HYSOL project. The simulation environment has been Dymola.

A. Startup operation

In this example, the gas turbine startup curves (exhaust temperature $T_{exh,out}$ and exhaust mass flow rate $\dot{m}_{gas}$) are depicted in the top part of Fig. 8 and in the bottom part of Fig. 9, respectively. At the beginning only the gas flows inside the HRS. When the outlet gas temperature reaches 300 °C, the HRS is filled with molten salts. At this moment, with the aim of reducing the startup time, the virtual afterheater is also turned on to reach the inlet gas temperature setpoint. The setpoint follows a ramp curve to avoid thermal stress in the HRS pipes. Once the molten salt mass flow rate is established to the nominal value, the temperature controller is activated to reach the nominal temperature at the molten salt outlet.

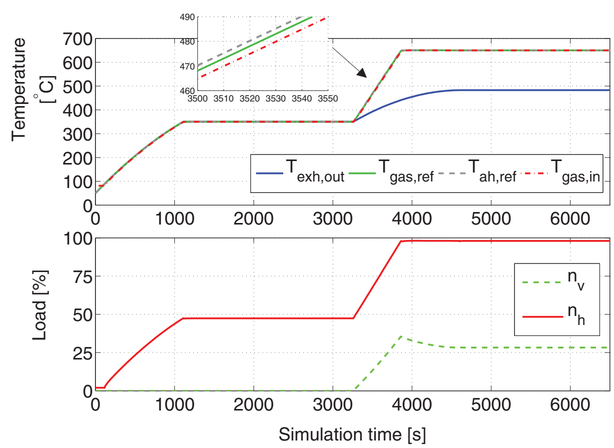

Fig. 8. Startup simulation. Virtual gas turbine variables.

B. Molten salt temperature control using the molten salt mass flow rate as control variable

Figure 10 shows an example of the molten salt temperature controller when the setpoint is established to the nominal value (560 °C) and different gas inlet temperatures are considered. The nominal value at the molten salt inlet temperature is considered (290 °C). This is a situation that will happen in the demonstrator to evaluate the behavior of

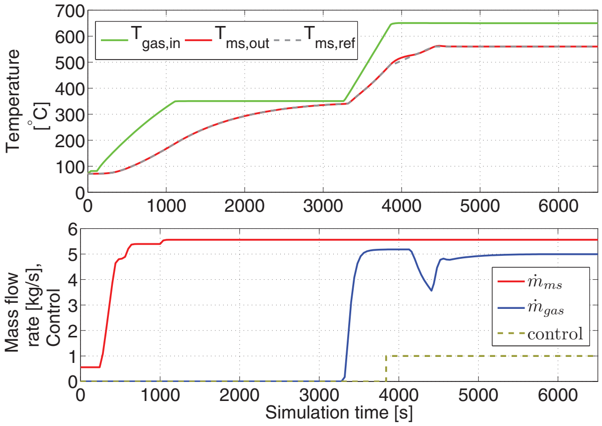

Fig. 9. Startup simulation. HRS variables.

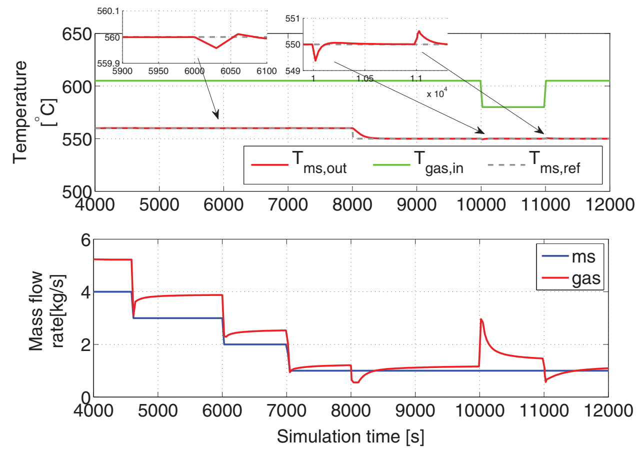

Fig. 11. Molten salt temperature control using a PI controller with feedforward action and gas mass flow rate as control variable.

the system when off-design tests will be performed. The master PI controller in the cascade configuration (Fig. 3) has been tuned with the following parameters: K_p=-3 kg/(s·°C), T_i=100 s and T_t=10 s.

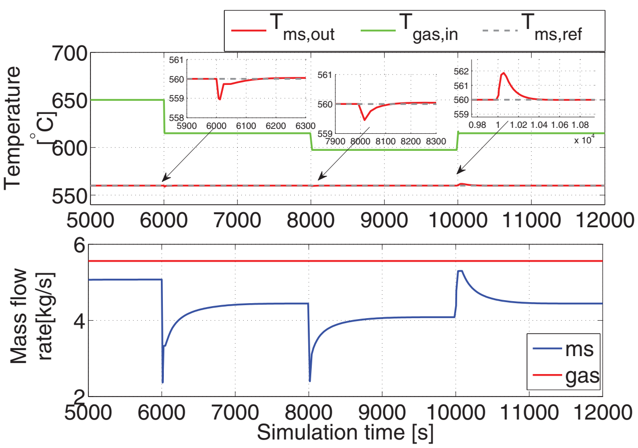

Fig. 10. Molten salt temperature control using a PI controller with feedforward action and molten salt mass flow rate as control variable.

C. Molten salt temperature control using the gas mass flow rate as control variable

An example of the molten salt temperature control when the gas flow rate is considered as the control variable is depicted in Fig. 11. The PI controller (Fig. 4) has been configured with the following parameters: K_p=-3 kg/(s·°C), T_i=100 s and T_t=10 s. In this case, different molten salt mass flow rates are considered (between 4 and 1 kg/s), the molten salt inlet temperature is 290 °C, the temperature setpoint changes at time 8000 s (from 560 °C to 550 °C) and a disturbance at the inlet gas temperature is simulated (it falls down 25 °C at time 10000 s). As it can be observed, the gas mass flow rate changes to maintain the molten salt temperature.

VI. CONCLUSIONS

To carry on the first experimental campaign at HYSOL demonstrator plant, basic control loops have been proposed to maintain the main variables at different operating points. Since the controllers have been only tested at simulation, a tuning phase is programmed at the experimental facility to obtain the desired system responses. First tests should be focused to validate the air heater model and evaluate the necessity of developing a collection of first-order models to cover the whole range of operating points. The HRS model and the heat balance proposed for the feedforward action must be also validated. The air-cooler controller performance and transport delays deserve special attention because they can affect severely to the controller designs presented in this paper. Moreover, the air heater controller response will be observed to reduce the startup if necessary. In that case, a predictive controller with a defined setpoint trajectory could be tested.

REFERENCES

[1] K. J.Åström, and T. Hägglund, PID controllers: theory, design, and tuning. Instrument Society of America, 1995.
[2] E. F. Camacho, M. Berenguel, F. R. Rubio, and D. Martínez, Control of solar energy systems. Springer Science & Business Media, 2012.
[3] S. C. Gülen and K. Kihyung, Gas Turbine Combined Cycle Dynamic Simulation: A Physics Based Simple Approach. J. Eng Gas Turb Power . vol. 136. 2013, pp. 011601-1–011601-15.
[4] M. Zhenjun and W. Shengwei, Energy efficient control of variable speed pumps in complex building central air-conditioning systems. Energy Build. vol. 41. 2009. pp. 197–205.
[5] R. Kehlhofer, B. Rukes, F. Hannemann and F. Stirnimann, Combined-cycle gas & steam turbine power plants. Pennwell, 2009.
[6] A. Tica, H. Guéguen, D. Dumur, D. Faille, and F. Davelaar, Hierarchical nonlinear model predictive control for combined cycle start-up optimization. In 51st Annual Conference on Decision and Control (CDC), 2012. pp. 2593–2598.
[7] C. S. Turchi, and Z. Ma, Co-located gas turbine/solar thermal hybrid designs for power production. Renew Energ. vol. 64. 2014, pp. 172–179.
[8] L. Valenzuela, E. Zarza, M. Berenguel, E. F. Camacho, Direct steam generation in solar boilers. IEEE Contr Syst Mag. vol. 24. 2004. pp. 15–29.